Enhanced thermoelectric figure of merit in nanostructured ZnO by nanojunction effect

Zi-Hua Wu, Hua-Qing Xie, and Yong-Biao Zhai

Citation: Applied Physics Letters **103**, 243901 (2013); doi: 10.1063/1.4842035
View online: http://dx.doi.org/10.1063/1.4842035
View Table of Contents: http://scitation.aip.org/content/aip/journal/apl/103/24?ver=pdfcov
Published by the AIP Publishing

Enhanced thermoelectric figure of merit in nanostructured ZnO by nanojunction effect

Zi-Hua Wu,[1] Hua-Qing Xie,[1,a)] and Yong-Biao Zhai[2]
[1]*School of Urban Development and Environmental Engineering, Shanghai Second Polytechnic University, Shanghai 201209, People's Republic of China*
[2]*Shanghai Yueda New Materials Science and Technology, Ltd., Shanghai 201209, People's Republic of China*

(Received 7 November 2013; accepted 21 November 2013; published online 9 December 2013)

We report in this letter the synthesis and thermoelectric properties of $Zn_{1-x}Ni_xO$/polyparaphenylene ($Zn_{1-x}Ni_xO$/PPP) organic-inorganic hybrid materials. Compared to the inorganic ZnO-based materials, hybrid materials exhibit dual effects of increased power factor consistent with the molecular junction effect and a reduction in thermal conductivity by the incorporation of conductive PPP. As a result, the greatest $ZT = 0.54$ of hybrid materials was obtained at 1173 K, which corresponds to a 6-fold enhancement compared to that of the best inorganic $Zn_{0.97}Ni_{0.03}O$ sample ($ZT = 0.09$) at 1000 K. © *2013 AIP Publishing LLC*. [http://dx.doi.org/10.1063/1.4842035]

Thermoelectric materials, which can be used for power generation by recovering waste heat and solid-state cooling devices, have been attracting a lot of attention due to their great potential for military and civilian applications. The conversion efficiency of thermoelectric devices can be characterized by the dimensionless figure of merit ZT, defined as $ZT = S^2\sigma T/(\kappa_L + \kappa_e)$, where σ is the electrical conductivity, S is the Seebeck coefficient (σS^2 is referred as power factor), κ_L is the lattice thermal conductivity, κ_e is the electron thermal conductivity, and T is the absolute temperature, respectively. The most efficient TE materials known to date are Bi_2Te_3 (Refs. 1–3) and PbTe,[4–6] but the related elements (Bi, Te, and Pb) are toxic or scarce. Therefore, nontoxic and low-cost ZnO becomes a promising candidate due to its excellent stability and lager Seebeck coefficient even though they display reduced ZT because of its high thermal conductivity and low electrical conductivity.[7–12]

Aside from the independent parameter κ_L, the other transport properties (S, σ, and κ_e) cannot be independently tuned due to the strong interdependence between each property via the carrier concentration in a given TE materials. As a result, the primary conventional effort for improving ZT is to reduce the lattice thermal conductivity κ_L.[13–15] A large number of researches have shown that incorporating nanostructure into bulk ZnO materials is an effective method to decrease κ_L. Since the electronic component of thermal conductivity κ_e is 100-fold lower than κ_L in ZnO, κ_L diminution directly translates to a lower κ. For example, Jood *et al.*[16] synthesized n-type Al-doped ZnO nanocomposites with a 20-fold lower κ_L than non-nanostructured ZnO and achieved a maximum $ZT = 0.44$ at 1000 K. However, the κ_L cannot be infinitely reduced because the phonon mean free path is larger than the interatomic distance.[17] Therefore, we should find an efficient method to enhance the power factor (σS^2) in order to further improve the ZT.

Polymer-inorganic hybrid nanomaterials are ideal in this regard due to the following mechanisms. First, they provide charge transport through discrete molecular orbitals, which give an opportunity to achieve the best efficiency in thermoelectric energy conversion.[18] Mahan and Sofo have already shown mathematically that σ and S can be optimized simultaneously through a single energy level.[19] Second, the drastic mismatch in the characteristic vibrational spectra between organic and inorganic can lower the vibrational heat conductance.[20] Therefore, we herein prepared $Zn_{1-x}Ni_xO$/polyparaphenylene nanoparticles by sol-gel method and then compressed nanoparticles into bulk material through spark plasma sintering. The microstructure and thermoelectric properties were further investigated.

The PPP was synthesized by polymerization of benzene in the presence of a catalyst, mixture of aluminum chloride ($AlCl_3$), and cuprous chloride dihydrous ($CuCl_2{\cdot}2H_2O$). 100 ml of benzene, 37.77 g of $AlCl_3$, and 24.14 g of $CuCl_2{\cdot}2H_2O$ were weighed and loaded into a three-necked, round-bottomed flask. The mixture was stirred and heated up to 40 °C for 2 h in an oil bath, then cooled to room temperature. After the reaction was complete, the slurry was filtered and washed some times and dried at 90 °C for 200 min in a drying oven. Finally, the sample was annealed at 900 °C for 5 h in an annealing furnace.

The $Zn_{1-x}Ni_xO$/PPP nanopowders were prepared by a sol-gel process. Appropriate amounts of zinc acetate [$Zn(CH_3COO)_2$] and nickel acetate [$Ni(CH_3COO)_2$] (for $Zn_{0.975}Ni_{0.025}O$ sample: 6.62 g of $Zn(CH_3COO)_2$ and 0.16 g of $Ni(CH_3COO)_2$; for $Zn_{0.95}Ni_{0.05}O$ sample: 6.47 g of $Zn(CH_3COO)_2$ and 0.32 g of $Ni(CH_3COO)_2$) were weighed and dissolved in diethylene glycol ($C_4H_{10}O_3$) solution to prepare 3 g of $Zn_{1-x}Ni_xO$. The mixture was stirred vigorously and heated to 165 °C. Then, the PPP powder was added into the mixture solution slowly and kept at 165 °C for 2 h. After gelation, rinsing, filtration, and drying, the nanocomposites powder was gained.

To study the thermoelectric properties, the powder with different content Ni and PPP was compressed by spark plasma sintering equipment (SPS-2040). All the samples were sintered at 1173 K under a pressure of 40 MPa in vacuum for 10 min. Then, $2 \times 2 \times 10\,mm^3$ bars and Φ $6 \times 1.5\,mm^2$ plates were cut to measure their thermoelectric properties. The phases of the prepared samples were characterized by X-ray diffraction (XRD) using Cu K_α radiation.

a)Electronic mail: hqxie@sspu.edu.cn

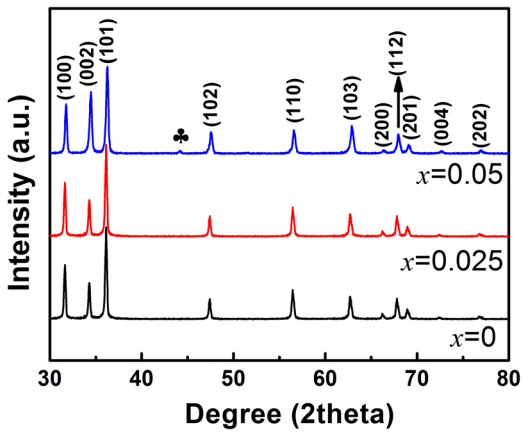

FIG. 1. XRD patterns of the Ni-doped ZnO samples ($x = 0$, 0.025, and 0.05).

Both electrical conductivity and Seebeck coefficient were measured simultaneously using ZEM-3 system. The thermal conductivity was calculated from the value of the thermal diffusivity (λ), density (ρ), and specific heat (C_p) using the relationship $\kappa = \lambda \rho C_p$, in which λ was measured using a laser flash system (FL-4100). In order to compare their properties, the synthesized samples were divided into two families: (1) $Zn_{0.975}Ni_{0.025}O$/PPP-family, including $Zn_{0.975}Ni_{0.025}O$, $Zn_{0.975}Ni_{0.025}O$/3%PPP, $Zn_{0.975}Ni_{0.025}O$/5%PPP, and $Zn_{0.975}Ni_{0.025}O$/9%PPP samples; (2) $Zn_{0.95}Ni_{0.05}O$/PPP-family, including $Zn_{0.95}Ni_{0.05}O$, $Zn_{0.95}Ni_{0.05}O$/3%PPP, $Zn_{0.95}Ni_{0.05}O$/5%PPP, and $Zn_{0.95}Ni_{0.05}O$ /9%PPP samples.

Figure 1 depicts the XRD patterns for the as-synthesized $Zn_{1-x}Ni_xO$ samples ($x = 0$, 0.025, and 0.05). A main crystalline phase appears on all the XRD patterns, which can be indexed as a hexagonal wurtzite structure of ZnO with the space group of P63mc (JCPDS 80-0075). For the lower Ni-concentration doping samples ($x \leq 0.025$), their XRD patterns appear only a pure hexagonal wurtzite phase. No detectable reflection from impurity can be found from the XRD patterns. However, when the Ni-doped concentration is higher than 0.025, although the wurtzite ZnO is still the main crystalline phase, some extra and faint diffraction peaks were observed. This impurity phase can be attributed to Zn_yNi_zO with cubic structure. Figures 2(a) and 2(b) show the transmission electron microscope (TEM) images of 9% PPP/$Zn_{0.95}Ni_{0.05}O$ bulk sample synthesized by SPS. We can see many of white nanoinclusions embedded in the matrix. The sizes of these white nanoinclusions are in the range of

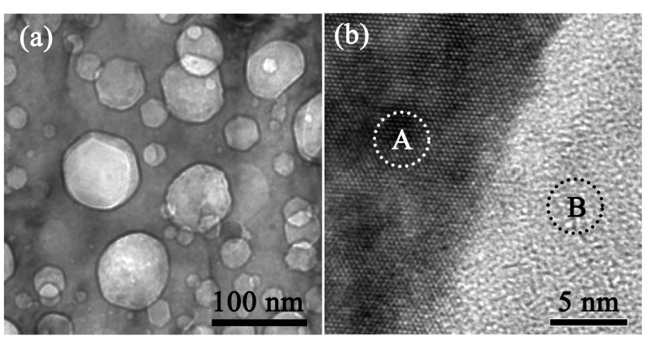

FIG. 2. TEM images of the 9% PPP/$Zn_{0.95}Ni_{0.05}O$ bulk sample (a) and interface structure of $Zn_{0.95}Ni_{0.05}O$ and PPP (b).

TABLE I. EDX analysis results of area A and area B.

Areas	Zn	O	Ni	C
A (at. %)	47.8	51.2	1	0
B (at. %)	5.7	6.3	0	88

10–70 nm. The energy dispersive spectrum (EDX) analysis (as shown in Table I) shows that white nanoinclusions (area B) exhibit a very strong peak of C in addition to a small amount of Zn and O, which indicates that the white nanoinclusions are PPP. While the matrix (area A) exhibits a very strong peak of Zn and O and only a small amount of Ni.

The electrical conductivity (σ) and Seebeck coefficient (S) of all the nanocomposites are shown in Figures 3(a) and 3(b), respectively. The addition of PPP nanoinclusions into $Zn_{1-x}Ni_xO$ results in an increase of carrier concentration and subsequent increase of electrical conductivity (σ) of the samples, except for $Zn_{0.975}Ni_{0.025}O$/9%PPP and $Zn_{0.95}Ni_{0.05}O$/9%PPP. The decrease in σ for $Zn_{0.975}Ni_{0.025}O$/9%PPP and $Zn_{0.95}Ni_{0.05}O$/9%PPP may be due to the decrease of carrier mobility. The behavior of S as a function of temperature is displayed in Figure 3(b). The negative value of S indicates that all the samples are n-type conductive, and the S decreases with increasing the temperature. The overall electrical properties are showed in Figure 3(c), which presents the power factor (σS^2) for the different nanocomposites as a function of the temperature. The highest power factor is obtained for the $Zn_{0.95}Ni_{0.05}O$/9%PPP nanocomposites with a value of $10.3 \times 10^{-4}\,Wm^{-1}\,K^{-2}$ at 1173 K. For the $Zn_{0.95}Ni_{0.05}O$/PPP family of the samples, 5 wt. % and 9 wt. % inclusion of PPP nanoparticles caused an approximately tripling of the electrical conductivity with only a 15%–20% reduction of Seebeck coefficient compared to the $Zn_{0.95}Ni_{0.05}O$ matrix, which amounts to a 300%–350% enhancement of power factor. Similarly, for $Zn_{0.975}Ni_{0.025}O$/PPP family of the samples, a 5 wt. % inclusion of PPP nanoparticles caused a near 7-fold increase in electrical conductivity only with a 30% reduction of Seebeck coefficient compared to the $Zn_{0.975}Ni_{0.025}O$ matrix, resulting in a substantial increase of power factor. This can be explained by molecular junction effect. Hybrid materials realize the combination of the discrete orbitals in the organic and the continuum states in the inorganic at inorganic-organic interface. This may cause a local increase in the density of the states over a narrow energy when the organic molecular orbitals (MOs) are well aligned with the chemical potential of the contacts. This phenomenon is similar to the single energy level transport envisioned by Mahan-Sofo theory.[19] The Seebeck coefficient of molecular junctions can be rewritten as[18]

$$S = G_S = \frac{\pi^2 k_B^2 T}{3e} \frac{2}{\mu - E_i}, \tag{1}$$

where G_S is the junction Seebeck coefficient, k_B the Boltzmann constant, μ the chemical potential of organic molecular orbital, and E_i the chemical potential of contacts. This expression shows that G_S can be rapidly increased when μ is approximately equal to E_i.

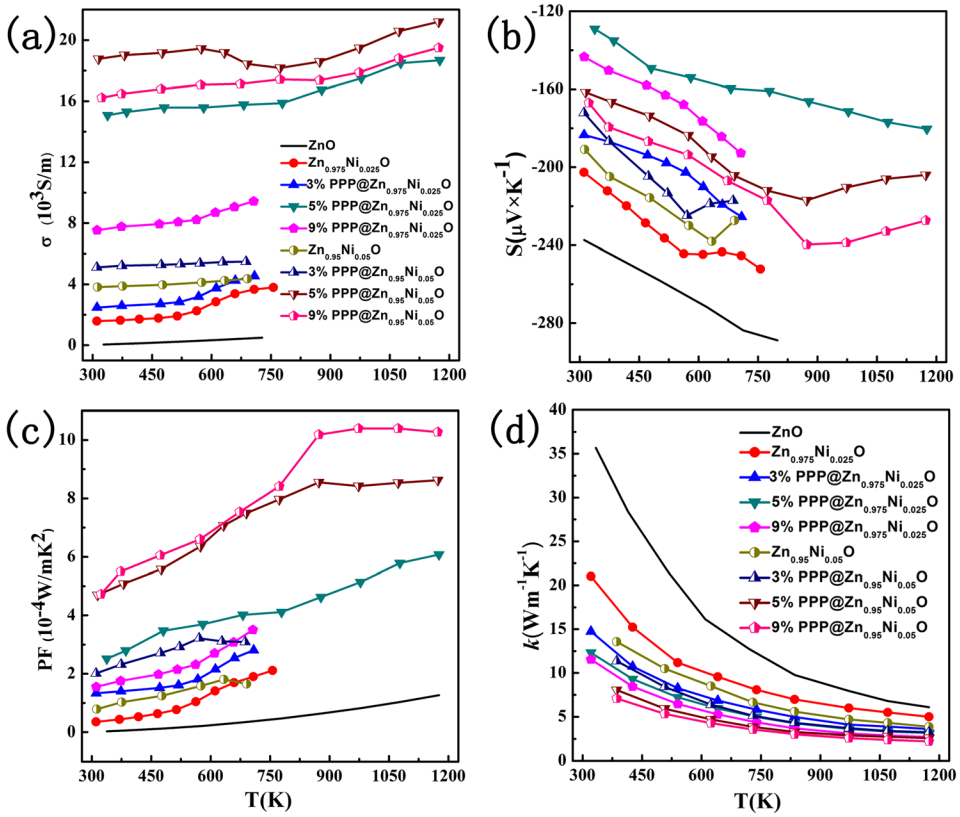

FIG. 3. Temperature dependence of electrical conductivity σ (a), Seebeck coefficient S (b), power factor PF (c), and thermal conductivity κ (d) for all the samples.

The temperature dependence of the thermal conductivity for all the nanocomposites is shown in Figure 3(d). Increasing concentration of PPP results in an almost uniform decrease of thermal conductivity over the entire temperature range. For $Zn_{0.975}Ni_{0.025}O$/PPP family of the samples, the thermal conductivity is reduced by approximately 25% with 3% PPP, by 35% with 5% PPP, and up to 40% with 9% PPP at 1173 K. Similarly, in $Zn_{0.95}Ni_{0.05}O$/PPP family of the samples, the decrease extent is 15%, 30%, and 40% at 1173 K, respectively. The depression of thermal conductivity should mainly attribute to three factors. First the drastic mismatch in characteristic vibrational spectra between organic PPP and inorganic ZnO can lower the vibrational heat conductance.[20] Second, the diameter of PPP particles is nanoscale, which can effectively scatter phonon.[21] Third, the phonons would be scattered effectively due to the interface imperfections and boundaries.[22,23] The temperature dependence of the thermoelectric ZT is shown in Figure 4. In all nanocomposites, the resulted increase in thermoelectric ZT is caused by an increase in power factor and the reduction in thermal conductivity. For the $Zn_{1-x}Ni_xO$ matrix, a large improvement in ZT is observed with 5% and 9% PPP. The highest $ZT \sim 0.54$ for $Zn_{0.95}Ni_{0.05}O$/9%PPP is obtained, which corresponds to a 10-fold enhancement compared to that of the $Zn_{0.95}Ni_{0.05}O$ matrix and is 6-fold higher than that of the $Zn_{0.97}Ni_{0.03}O$ ($ZT \sim 0.09$/1000 K) reported by Colder *et al.*[24]

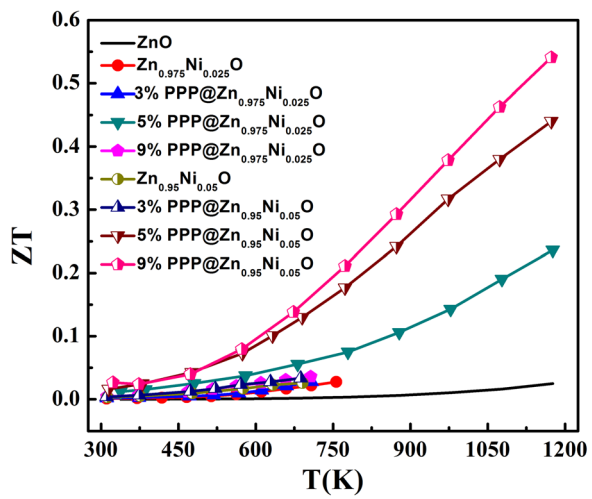

FIG. 4. Temperature dependent ZT value of the sintered bulk hybrid materials.

In summary, the $Zn_{1-x}Ni_xO$/PPP nanopowder was synthesized by sol-gel method, and then nanopowder was compressed into bulk thermoelectric material. The presence of PPP nanoparticles in $Zn_{1-x}Ni_xO$ matrix is found to be effective in improving ZT by the dual effects of increased power factor consistent with the molecular junction effect and a reduction in thermal conductivity. As a result, the maximum $ZT \sim 0.54$ is obtained, which is 6-fold higher than that of the $Zn_{0.97}Ni_{0.03}O$ sample fabricated by the same method.

This study was supported by the National Natural Science Foundation of China (Grant No. 51206103), the Innovation Program of Shanghai Municipal Education Commission (Grant No. 13YZ128), and the Program for Professor of Special Appointment (Eastern Scholar) at Shanghai Institutions of Higher Learning.

[1]B. Poudel, Q. Hao, Y. Ma, Y. Lan, A. Minnich, B. Yu, X. Yan, D. Wang, A. Muto, D. Vashaee, X. Chen, J. Liu, M. S. Dresselhaus, G. Chen, and Z. Ren, Science **320**, 634 (2008).

[2]X. B. Zhao, X. H. Ji, Y. H. Zhang, T. J. Zhu, J. P. Tu, and X. B. Zhang, Appl. Phys. Lett. **86**, 062111 (2005).
[3]X. Tang, W. Xie, H. Li, W. Zhao, and Q. Zhang, Appl. Phys. Lett. **90**, 012102 (2007).
[4]J. P. Heremans, V. Jovovic, E. S. Toberer, A. Saramat, K. Kurosaki, A. Charoenphakdee, S. Yamanaka, and G. J. Snyder, Science **321**, 554 (2008).
[5]Y. Pei, X. Shi, A. LaLonde, H. Wang, L. Chen, and G. J. Snyder, Nature **473**, 66 (2011).
[6]Y. Pei, A. D. LaLonde, N. A. Heinz, X. Shi, S. Iwanaga, H. Wang, L. Chen, and G. J. Snyder, Adv. Mater. **23**, 5674 (2011).
[7]K. H. Jung, K. H. Lee, W.-S. Seo, and S.-M. Choi, Appl. Phys. Lett. **100**, 253902 (2012).
[8]K. Kim, P. C. Debnath, D. H. Lee, S. Kim, and S. Y. Lee, Nanoscale Res. Lett. **6**, 552 (2011).
[9]D. Lin, H. Wu, X. Qin, and W. Pan, Appl. Phys. Lett. **95**, 112104 (2009).
[10]Q. Wan, Z. Xiong, J. Dai, J. Rao, and F. Jiang, Opt. Mater. **30**, 817 (2008).
[11]J. Fan and R. Freer, J. Appl. Phys. **77**, 4795 (1995).
[12]M. Ohtaki, T. Tsubota, K. Eguchi, and H. Arai, J. Appl. Phys. **79**, 1816 (1996).
[13]L. D. Hicks and M. S. Dresselhaus, "Thermoelectric figure of merit of a one-dimensional conductor," Phys. Rev. B **47**, 16631 (1993).
[14]T. C. Harman, P. J. Taylor, M. P. Walsh, and B. E. Laforge, Science **297**, 2229 (2002).
[15]W. Xie, J. He, H. J. Kang, X. Tang, S. Zhu, M. Laver, S. Wang, J. R. Copley, C. M. Brown, Q. Zhang, and T. M. Tritt, Nano Lett. **10**, 3283 (2010).
[16]P. Jood, R. J. Mehta, Y. Zhang, G. Peleckis, X. Wang, R. W. Siegel, T. Borca-Tasciuc, S. X. Dou, and G. Ramanath, Nano Lett. **11**, 4337 (2011).
[17]H. J. Goldsmid, *Introduction to Thermoelectricity* (Springer, Berlin, 2010).
[18]J. A. Malen, S. K. Yee, A. Majumdar, and R. A. Segalman, Chem. Phys. Lett. **491**, 109 (2010).
[19]G. D. Mahan and J. O. Sofo, Proc. Natl. Acad. Sci. U.S.A. **93**, 7436 (1996).
[20]D. G. Cahill, W. K. Ford, K. E. Goodson, G. D. Mahan, A. Majumdar, and H. J. Maris, J. Appl. Phys. **93**, 793 (2003).
[21]E. T. Swartz and R. O. Pohl, Rev. Mod. Phys. **61**, 605 (1989).
[22]R. Y. Wang, R. A. Segalman, and A. Majumdar, Appl. Phys. Lett. **89**, 173113 (2006).
[23]C. Dames and G. Chen, *Thermoelectrics Handbook: Macro to Nano*, edited by D. M. Rowe (Taylor and Francis Group, Boca Raton, FL, 2006).
[24]H. Colder, E. Guilmeau, C. Harnois, S. Marinel, R. Retoux, and E. Savary, J. Eur. Ceram. Soc. **31**, 2957 (2011).